



3 1176 00134 0182

NASA TM-78810

NASA Technical Memorandum 78810

NASA-TM-78810 19790012168

METASTABLE SOUND SPEED IN GAS-LIQUID MIXTURES

Joseph W. Bursik, Rensselaer Polytechnic Institute

and

Robert M. Hall, NASA Langley Research Center

FOR REFERENCE

NOT TO BE TAKEN FROM THE ROOM

March 1979

LIBRARY COPY

LANGLEY RESEARCH CENTER
HAMPTON, VIRGINIA



National Aeronautics and
Space Administration

Langley Research Center
Hampton, Virginia 23665

METASTABLE SOUND SPEED IN GAS-LIQUID MIXTURES

Joseph W. Bursik* and Robert M. Hall

Langley Research Center

SUMMARY

Acoustic measurements in air-water mixtures at a fixed temperature and pressure in which void fraction is varied yield a sound speed curve as a function of void fraction exhibiting a minimum in the vicinity of a void fraction of one half. A metastable theory in which the entropies of the mixture, gas phase, and liquid phase are individually held constant yields a corresponding curve whose minimum sound speed is about 20% higher than the measured value. When an ad hoc modification is made which replaces isentropic by isothermal propagation the new theoretical minimum region is brought into agreement with experiment; however, the boundary values of the sound speed at void fractions of zero and unity are no longer the usual isentropic sound speeds for pure water and pure air. In this paper a new metastable theory is developed. By imposing only constant mixture entropy and phase composition during propagation, the new theory successfully predicts both the minimum region and the end points. The theory produces a heat capacity ratio for the mixture which self-adjusts to both normal values for the pure phases and to values near unity for a broad range of void fraction values about the minimum in the curve. The new theory is extended to single-component pure substances including para-hydrogen and nitrogen with emphasis on the latter.

*Associate Professor of Mechanical Engineering, Aeronautical Engineering, and Mechanics, Rensselaer Polytechnic Institute, Troy, New York.

INTRODUCTION

A large transonic wind tunnel is under construction at the Langley Research Center. This new National Transonic Facility (NTF) will use a relatively novel concept to achieve high Reynolds numbers - liquid nitrogen is injected directly into the nitrogen test gas and the resulting evaporation of the liquid cools the test gas to cryogenic temperatures approaching liquid-vapor saturation temperatures (see references 1-3). In support of this new wind tunnel, studies have been undertaken at Langley to insure that the low temperature behavior of the nitrogen test gas is sufficiently understood to guarantee its usefulness for transonic aerodynamic testing (see references 4 and 5).

The present study involves the calculation of sound speed for a gas-liquid mixture. In cryogenic tunnels such as the NTF, two-phase flow is always present at the liquid nitrogen injection station, and at times may be desired in the test section in the form of fog droplets for the purpose of flow visualization or for seeding for laser velocimetry. While the gas-liquid mixtures in cryogenic nitrogen tunnels are expected to involve mostly gas - vapor mass fraction generally greater than 0.98 at the injection station and close to 1.00 in areas of seeding - the general sound speed literature used in this paper deals with mixtures of air-water and steam-water that are mostly liquid. Nevertheless, the literature can be used to develop the theory that will apply to cryogenic nitrogen tunnels. The present paper will consider these water mixtures before addressing gas-liquid nitrogen. All nitrogen calculations will use thermodynamic properties from reference 6.

SYMBOLS

a_0	equilibrium, zero-frequency, two-phase, sound speed, m/sec
a_1	metastable, two-phase sound speed, defined by equation (32), m/sec
a_2	metastable, ad-hoc, two-phase sound speed, defined by equation (7), m/sec
a_3	metastable, triply isentropic, two-phase sound speed, defined by equation (4), m/sec
C_V	constant volume specific heat capacity, J/(kg-K)
C_P	constant pressure specific heat capacity, J/(kg-K)
P	pressure, N/m ²
s	specific entropy, J/(kg-K)
r	non-dimensional correlation parameter defined in equation (39)
R	specific gas constant, J/(kg-K)
T	temperature, K
v	specific volume, m ³ /kg
x	vapor mass fraction (quality)
x_0	value of quality for which $(\partial s / \partial T)_x$ is zero
α	void fraction, fraction of vapor volume to the total volume
γ	specific heat ratio (C_P / C_V)
ρ	density, kg/m ³

Subscripts

c	pertaining to the critical point
G	denoting gas (vapor) phase

L denoting liquid phase

T denoting isothermal value

BACKGROUND

Propagation of sound in two-phase, gas-liquid systems has undergone extensive theoretical and experimental study. One of the earliest expressions for this acoustic velocity comes from the so-called isentropic, homogeneous equilibrium model (IHE) in which average equilibrium properties are used in conjunction with the assumption of total phase equilibrium to describe sound propagation when the two-phases are finely interspersed in one another. In this paper, this velocity of sound is denoted by a_o and it is computed only for nitrogen. Details of the a_o computation are omitted because, first, it is such a widely known model and, second, the subsequent main thrust of the paper will deal with metastable models. As usual, the square of a_o is taken as $(\partial P / \partial \rho)_s$ and this quantity is evaluated herein at equilibrium two-phase states for nitrogen using a computer program generated at the Langley Research Center from reference 6.

One of the chief characteristics of a_o is associated with the manner in which an isentrope crosses the phase boundary as it passes from the one-phase region (liquid or vapor) into the two-phase region of a P, ρ property diagram where the saturated liquid and vapor curves are distinct and separate (in contrast to a P, T plane of properties where the saturated liquid and vapor curves coalesce into a single curve). In the P, ρ plane the isentrope crosses a phase boundary with discontinuous slope; that is $(\partial P / \partial \rho)_s$ has two values at a point on the phase boundary. If this partial derivative is interpreted as the sound speed, then, from a total equilibrium point of view, there are two values of the sound speed at a point of the phase boundary. (As will be seen

later, it is possible to avoid having two sound speeds at a single point of the phase boundary by introducing metastable effects into the two-phase propagation of sound. The two-phase, equilibrium $(\partial P / \partial \rho)_s$ is then simply a thermodynamic partial derivative to which no further physical attribute is assigned.) Furthermore, the formula for a_o will not yield the usual single-phase velocity of sound at either the liquid or the vapor boundary. If the boundary values of a_o are denoted by $a_{o,L}$ on the liquid side and $a_{o,G}$ on the vapor side and if the usual single-phase sound speeds are denoted by a_L and a_G - all in meters per second - then this discontinuous boundary behavior for the IHE model can be illustrated for nitrogen in the table that follows:

T (K)	SATURATED LIQUID LIMIT		SATURATED VAPOR LIMIT	
	ONE-PHASE a_L	TWO-PHASE $a_{o,L}$	ONE-PHASE a_G	TWO-PHASE $a_{o,G}$
80	894	3.75	177	163
100	613	16.8	183	167
120	338	49	176	139

The discontinuity is consistently weaker on the vapor side, with the strongest discontinuity occurring on the saturated liquid side at a temperature of 80 K where $a_{o,L}$ is an incredibly small 3.75 meters per second. Normally, the boundary sound speed associated with the single-phase side is the one recognized as the actual boundary acoustic velocity.

For example, when using the saturation tables in reference 6, it is tacitly understood that these boundary values are to be taken as the normal single-phase values. In the case of water, this discontinuity is discussed in reference 7, and a_o is plotted isothermally as a function of void fraction in figure 1 of reference 8 and again shows liquid phase values close to zero.

In addition to the (IHE) model, various non-equilibrium models have also been developed. One of these introduces a non-equilibrium feature by neglecting changes in phase composition during passage of the sound wave. As with a_o , the basic sound speed expression used is

$$a = [-v^2/(\partial v/\partial P)_s]^{1/2} \quad (1)$$

where

$$v = (1-x) v_L + x v_G \quad (2)$$

with x being the vapor mass fraction (quality) and v_L and v_G the liquid and vapor specific volumes. While both the (IHE) and non-equilibrium models assume constant mixture entropy for the wave propagation, the latter model also assumes constant liquid phase entropy as well as constant gas phase entropy; that

is, s , s_L , and s_G are all individually constant during the passage of the sound wave as is the quality. With these assumptions equation (2) is differentiated into

$$\left(\frac{\partial v}{\partial P}\right)_s = (1 - x) \left(\frac{\partial v}{\partial P}\right)_{s,L} + x \left(\frac{\partial v}{\partial P}\right)_{s,G} \quad (3)$$

The partial derivatives on the right hand side of this equation are respectively replaced by $(-v_L^2/a_L^2)$ and $(-v_G^2/a_G^2)$, and the resulting expression is substituted into equation (1) to give the metastable, triply isentropic, $(M, 3s)$ sound speed as

$$a_3 = v / \{ (1 - x)(v_L/a_L)^2 + x(v_G/a_G)^2 \}^{1/2} \quad (4)$$

Here, a_L and a_G are the isentropic, single-phase boundary values. This equation is used by Karplus (reference 7), Wood (reference 8), and Dvornichenko (reference 9) in a form that substitutes vapor void fraction for quality. In reference 10, Wallis generalizes the isentropic phase constraints used in defining a_L and a_G to permit other acoustical vibrational constraints such as isothermal phase propagation to be introduced into the theory of sound

propagation. When these constraints are the same as in this section, his equation (2.46) is identical with equation (4) above, and his equation (2.50), with the void fraction replacing the quality, is identical with the equations derived in references 7-9.

The important features of this (M,3s) model are summarized below:

(1) In contrast to the (IHE) model, the acoustic velocity of the (M,3s) model reduces to the usually measured single-phase velocities for $x = 0$ and $x = 1$. With a_0 used to denote the sound speed associated with the (IHE) model, and with a_3 used to denote (M,3s) sound speed, the boundary value comparison in meters per second for the two models using nitrogen at 100K gives

$$\begin{array}{ll} a_{0,L} = 16.8 & a_{3,L} = 613 \\ a_{0,G} = 167 & a_{3,G} = 183 \end{array}$$

(2) When sound speed is plotted against quality at constant temperature and pressure using the (M,3s) model, the resulting curve exhibits a minimum with the minimum sound speed being smaller than either boundary value. For nitrogen at 100 K the minimum velocity of sound is about 77 meters per second and occurs very close to the saturated liquid boundary at a quality of about 0.049. (As will be shown later, the (IHE) model predicts a monotonic curve.) Measured data for the two-component air-water mixture also shows a similar minimum (reference 7 and reference 10, p. 266) and a similar pattern holds for measurements on a single-component steam-water system as shown in reference 11.

While qualitatively correct, the (M,3s) model overpredicts the minimum sound speed in the air-water system of Wallis (reference 10, figure 9.12) by approximately 20%. In order to account for this discrepancy, Karplus (reference 7) first transforms equation (4) to replace quality by void fraction and then makes an ad hoc modification in the (M,3s) model by replacing isentropic propagation in the phases by isothermal propagation; that is, he permits heat transfer between the phases. Actually Karplus did not concern himself with the liquid phase isothermal modification because two further approximations, $\rho_L \gg \rho_G$ and $\rho_L a_L^2 \gg \rho_G a_G^2$, enable him to transform equation (4) into

$$a_3^2 \approx a_G^2 \rho_G / \{\rho_L \alpha(1 - \alpha)\} \quad (5)$$

where α is the void fraction. In this form the question of isentropic versus isothermal propagation for the individual phases is not yet addressed; however, since all reference to the liquid phase velocity of sound has been eliminated, no isothermal substitution for isentropic propagation need be made for the liquid. For atmospheric air at room temperature an ideal gas substitution can be made for the gas phase speed of sound according to $a_G^2 = \gamma RT$ if isentropic, or simply RT , if isothermal. Choice of the latter then yields the following equation after using $P = \rho RT$,

$$a_2^2 \approx P[\rho_L \alpha(1 - \alpha)]^{-1} \quad (6)$$

for an isothermally modified model (M,s,2T) for which a_2 now represents isothermal sound propagation in both phases even though the approximate equation (6) only involves the gas phase sound speed. The single s is retained in the classification notation on the assumption that Karplus models the mixture as isentropic. Without using the above two Karplus approximations concerning the magnitudes of sound speeds and densities, the (M,s,2 T) sound speed may also be formed from equation (4) by the appropriate isothermal substitutions of $a_{L,T}$ for a_L and $a_{G,T}$ for a_G . Then, with these new symbols representing $\{-v^2(\partial P/\partial v)_T\}$ respectively evaluated at the saturated liquid and vapor boundaries,

$$a_2 = v/\{(1 - x)(v_L/a_{L,T})^2 + x(v_G/a_{G,T})^2\} \quad (7)$$

The significant results of this modified, ad hoc, (M,s,2T) theory are:

(1) It correctly predicts the magnitude of the sound speed in the minimum point region in the Karplus experiments (reference 7), which are also shown in Wallis (reference 10, p. 266).

(2) Equation (7) for the isothermal, two-phase, sound speed does not yield the usual single-phase, isentropic sound speeds at the boundary

points $x = 0$ and $x = 1$, or $\alpha = 0$ and $\alpha = 1$. (The approximate equation (6) gives boundary velocities that are both infinite, but Karplus indicates negligible error in the use of equation (6) for $0.002 < \alpha < 0.94$.)

The difference between isentropic and isothermal propagation is negligible for pure-phase water at room temperature because the ratio of heat capacities is close to unity. However, pure-phase air, treated as an ideal gas with a heat capacity ratio of $\gamma = 1.4$, will have a ratio of isentropic to isothermal sound speed of $\sqrt{1.4} = 1.183$ and, coincidentally, this is about the same order of magnitude difference as the original overprediction of the minimum sound speed inherent in the (M,3s) model. The features of the air-water system are shown in figure 1 where the sound speeds a_3 and a_2 , corresponding respectively to the (M,3s) and (M,s,2T) models of equations (4) and (7) are plotted. Discussion of the third curve, a_1 , will come later. In the computation, air was treated as an ideal gas and the water data were taken from reference 12. Wallis in reference 10, page 266, shows experimental data for the air-water system at a similar temperature along with the corresponding theoretical lines. A reproduction of his figure 9.12 is shown herein as figure 2. The line labeled by Wallis as "isothermal" corresponds to the (M,s,2T) model, a_2 , and his line labeled "adiabatic" corresponds to the (M,3s) model, a_3 .

Because of the steeply rising curves on the gas side of figure 1 where the void fraction is close to one, the difference in the gas boundary values of the sound speeds for isothermal and isentropic propagation is obscured. In order to illustrate these differences better and also to emphasize the mass dominance of the liquid phase in the vicinity

of the minimum point, the void fraction, α , is transformed to the quality, x , by use of

$$x = \alpha v_L / \{v_G - \alpha(v_G - v_L)\} \quad (8)$$

Then the same sound speeds, a_2 and a_3 , are replotted in figure 3. Now the $x = 1$ values of a_2 and a_3 are clearly evident, as is the mass dominance of the liquid phase. The minima in figure 1 show a rough balance between liquid and vapor volumes; that is, the value of the void fraction that minimizes any one of the curves is about 1/2. Indeed, the approximate form of a_2 from equation (6) has its minimum exactly at a void fraction of 1/2. In figure 3, the previous, apparent balance between the phases is completely eliminated as the minima are crowded against the pure liquid axis. This reflects the enormous density difference between water and air. Again, discussion of the a_1 curve is deferred.

Further complications in matching theory and data are introduced by Semenov and Kosterin in reference 11. In contrast to the data shown by Wallis, their measurements on single-component steam-water systems give results in apparent quantitative agreement with the basic, unmodified (M,3s) theory. At first, their results may suggest a fundamental distinction between single- and two-component two-phase systems. On the

other hand, the uncertainty in their acoustic velocity measurements was reported to be $\pm 9\%$, and this may be sufficiently large to obscure the possible differences between the data and the (M,3s) theory.

In view of these conflicting experimental results and theoretical models, a new metastable theory of sound propagation in two-phase systems was sought which would predict the correct minimum in the acoustic velocity-void fraction curve as does the (M,s,2T) model and would achieve isentropic single-phase velocities at $x = 0$ and $x = 1$ as does the (M,3s) theory. The new approach retains two key concepts of the (M,3s) theory, - that a local acoustic disturbance is again assumed to propagate in a homogeneous two-phase mixture.

(1) without phase change,

(2) at constant mixture entropy.

These postulates make the metastability similar to isentropic expansion of a super-heated vapor in a nozzle to a pressure less than saturation without condensation occurring immediately. In this well known case, only the gas phase is present at the onset of the metastability; whereas, metastable propagation of sound in a homogeneous two-phase mixture has the added complexity of requiring a similar non-equilibrium effect for each phase at the onset of metastability. At this point the new theory drops the (M,3s) additional requirements of constant s_L and s_G for a different concept of metastability described in the next section.

METASTABILITY

In order to develop a new description of two-phase metastability from the stated postulates, the total differential of the entropy function for a single phase is taken from

thermodynamics and written for each phase as

$$ds_L = \frac{C_{P,L}}{T} dT - \left(\frac{\partial v}{\partial T}\right)_{P,L} dP \quad (9)$$

and

$$ds_G = \frac{C_{P,G}}{T} dT - \left(\frac{\partial v}{\partial T}\right)_{P,G} dP \quad (10)$$

For a saturated two-phase system of one component, these two differentials are expanded about two different states, each at the same temperature and pressure. One of these states corresponds to the saturated liquid, and the other, to saturated vapor. Let these states be the ones shown as points L and G in the sketch of figure 4(a) which shows a pair of isobars at P and P+dP passing from the liquid region into the two-phase region and finally into the vapor region. L' and G' are respectively saturated liquid and vapor states at the lower isobar. Starting from the point L and assuming an isentropic expansion occurs which drops the pressure ($dP < 0$), total phase equilibrium - including phase change - requires the expansion to terminate at the two-phase point

marked as A. Similarly, an isentropic acoustic expansion from G would terminate as the two-phase state B.

In order to impose the condition $dx = 0$ during the wave passage, penetration into the two-phase region must be avoided. To make this possible, a second sheet of metastable-unstable properties is assumed to underlay the normal two-phase equilibrium property sheet. For purposes of discussion it is sketched in figure 4(b) in a manner similar to a van der Waals metastable-unstable region. Here the usual equilibrium isobars are shown as solid lines P and $P+dP$ with L, L', G, G' being the same former saturation states. The dashed curves represent one-phase, metastable-unstable continuations of these isobars. Now the passage of a disturbance ($dP < 0$) from the isothermal and isobaric points L and G without phase change shifts these points to the new isobar $P + dP$ such that the final phase points have the same (and new) final temperature. For the way figure 4(b) is sketched it is impossible for the individual phase points to shift about local isentropes passing through L and G and satisfy the final isothermal condition. If this sketch were a true representation of thermodynamic properties, the (M,3s) theory of sound propagation could not possibly be valid. On the other hand, it is possible of course to alter the sketching of the isobar $P + dP$ such that the pair of local isentropic expansions emanating from L and G end on the $P + dP$ isobar with the same temperature in conformity with at least this portion of the (M,3s) theoretical requirements. Obviously, the thermodynamic pattern of properties is rigidly set, and any theory of two-phase sound propagation must conform to this pattern. Later, such a conformance test will be derived for the (M,3s) model which, when tested for several substances

including nitrogen, indicates that this model is invalid with respect to the thermodynamic data used. For the present, it suffices that the two sketches indicate the potential metastable thermodynamic states which can be associated with two-phase sound propagation.

DERIVATION OF THE NEW EQUATION

In the derivation of the new equation for metastable sound propagation the basic starting point is again equation (1), and this means finding a way of evaluating $(\partial v / \partial P)_g$. Likewise, the mixture specific volume continues to be described by equation (2), and it is perturbed by the passage of the wave to give

$$dv = (1 - x) dv_L + x dv_G \quad (11)$$

since propagation is again assumed to occur without phase change. The single-phase specific volumes are ordinarily functions of temperature and pressure whose total differentials are

$$dv_L = \left(\frac{\partial v}{\partial T} \right)_{P,L} dT + \left(\frac{\partial v}{\partial P} \right)_{T,L} dP \quad (12)$$

and

$$dv_G = \left(\frac{\partial v}{\partial T}\right)_{P,G} dT + \left(\frac{\partial v}{\partial P}\right)_{T,G} dP \quad (13)$$

where dT and dP are the same in both equations and are the perturbations associated with the sound wave. Substitution of the last two equations into the preceding one gives

$$dv = \left(\frac{\partial v}{\partial T}\right)_P dT + \left(\frac{\partial v}{\partial P}\right)_T dP \quad (14)$$

where the mixture quantities $(\partial v/\partial T)_P$ and $(\partial v/\partial P)_T$ are given by

$$\left(\frac{\partial v}{\partial T}\right)_P = (1 - x) \left(\frac{\partial v}{\partial T}\right)_{P,L} + x \left(\frac{\partial v}{\partial T}\right)_{P,G} \quad (15)$$

and

$$\left(\frac{\partial v}{\partial P}\right)_T = (1 - x) \left(\frac{\partial v}{\partial P}\right)_{T,L} + x \left(\frac{\partial v}{\partial P}\right)_{T,G} \quad (16)$$

For later use, the third partial derivative of the equation of state is formed in the usual way to give

$$\left(\frac{\partial P}{\partial T}\right)_v = - \left(\frac{\partial v}{\partial T}\right)_P / \left(\frac{\partial v}{\partial P}\right)_T \quad (17)$$

Since the problem is to form $(\partial v / \partial P)_s$, the mixture entropy is now introduced as

$$s = (1 - x) s_L + x s_G \quad (18)$$

and differentiated without phase change to give

$$ds = (1 - x) ds_L + x ds_G \quad (19)$$

The quantities ds_L and ds_G are eliminated by use of equations (9) and (10) to give

$$ds = \frac{C_P}{T} dT - \left(\frac{\partial v}{\partial T}\right)_P dP \quad (20)$$

where C_P is defined for the mixture as

$$C_P = (1 - x) C_{P,L} + x C_{P,G} \quad (21)$$

and $(\partial v / \partial T)_P$ has been previously defined in equation (15). It is noted that the heat capacity is the usual $T(\partial s / \partial T)_P$ and is not infinite in the metastable theory. This is contrary to its infinite behavior in stable two-phase theory for pure substances.

Now all that is required to form $(\partial v / \partial P)_S$ is to change the independent variables in equation (20) from dT and dP to dv and dP . This is accomplished by rewriting the equation of state by substituting equation (17) into equation (14). This gives

$$dT = \left(\frac{\partial T}{\partial P} \right)_v dP + \left(\frac{\partial T}{\partial v} \right)_P dv \quad (22)$$

and this is used to eliminate dT in equation (20) with the result that

$$ds = \frac{C_P}{T} \left(\frac{\partial T}{\partial v} \right)_P dv + \left\{ \frac{C_P}{T} \left(\frac{\partial T}{\partial P} \right)_v - \left(\frac{\partial v}{\partial T} \right)_P \right\} dP \quad (23)$$

From this, the partial derivative $(\partial P/\partial v)_s$ is read as

$$\left(\frac{\partial P}{\partial v}\right)_s = - \frac{C_P \left(\frac{\partial T}{\partial v}\right)_P}{C_P \left(\frac{\partial T}{\partial P}\right)_v - T \left(\frac{\partial v}{\partial T}\right)_P} \quad (24)$$

Multiplying numerator and denominator by $(\partial P/\partial T)_v$ and then using equation (17) in the numerator gives

$$\left(\frac{\partial P}{\partial v}\right)_s = \frac{C_P \left(\frac{\partial P}{\partial v}\right)_T}{C_P - T \left(\frac{\partial P}{\partial T}\right)_v \left(\frac{\partial v}{\partial T}\right)_P} \quad (25)$$

In stable one-phase thermodynamics the denominator would be the heat capacity at constant volume. To test this, the equation of state is rewritten as

$$dP = \left(\frac{\partial P}{\partial T}\right)_v dT + \left(\frac{\partial P}{\partial v}\right)_T dv \quad (26)$$

and this is used to eliminate dP in equation (20). The result is

$$ds = \left\{ \frac{C_P}{T} - \left(\frac{\partial v}{\partial T} \right)_P \left(\frac{\partial P}{\partial T} \right)_v \right\} dT - \left(\frac{\partial P}{\partial v} \right)_T \left(\frac{\partial v}{\partial T} \right)_P dv \quad (27)$$

From its basic definition,

$$C_v = T \left(\frac{\partial s}{\partial T} \right)_v \quad (28)$$

Therefore, it follows from the last two equations that

$$C_v = C_P - T \left(\frac{\partial v}{\partial T} \right)_P \left(\frac{\partial P}{\partial T} \right)_v \quad (29)$$

and, from equations (25) and (29)

$$\left(\frac{\partial P}{\partial v} \right)_s = \gamma \left(\frac{\partial P}{\partial v} \right)_T \quad (30)$$

where

$$\gamma = C_P / C_v \quad (31)$$

When equation (30) is substituted into equation (1), the final form of the acoustic velocity, now designated as a_1 , becomes

$$a_1 = [-\gamma v^2 / (\partial v / \partial P)_T]^{1/2} \quad (32)$$

In summary, the expression for a_1 in equation (32) represents the new metastable equation. It has assumed no phase transition during an acoustic disturbance and has assumed that the total entropy of the system (not of the individual phases) remains constant. As will be shown, the values of a_1 reduce to the respective single-phase values of sound speeds in the limits of all liquid or all gas.

For computational purposes one must know the ordinary single-phase values of $C_{P,L}$, $C_{P,G}$, $C_{V,L}$, $C_{V,G}$, $(\partial v / \partial T)_{P,L}$, $(\partial v / \partial T)_{P,G}$, $(\partial v / \partial P)_{T,L}$, $(\partial v / \partial P)_{T,G}$, v_L , and v_G in order to obtain a sound speed versus either quality or void fraction curve at a given temperature and pressure. In conjunction with this, it is noted that the right side of equation (21) reduces to the ordinary single-phase heat capacities at $x = 0$ and $x = 1$. A similar reduction occurs at these qualities for $(\partial v / \partial T)_P$ and $(\partial v / \partial P)_T$ as is evident in equations (15) and (16). Substitution of equation (17) in equation (29) gives an alternate form of the constant volume heat capacity as

$$C_v = C_p + T(\partial v / \partial T)_P^2 / (\partial v / \partial P)_T \quad (33)$$

At $x = 0$ this reduces to the usual single-phase form

$$C_{V,L} = C_{P,L} + T(\partial v / \partial T)_{P,L}^2 / (\partial v / \partial P)_{T,L} \quad (34)$$

A similar reduction occurs at $x = 1$. Finally, equation (8) or the alternate form

$$\alpha = x v_G / v \quad (35)$$

can be used to convert quality into void fraction or vice versa.

RESULTS AND DISCUSSION

Two-Component System

Referring back to figures 1 and 3 for the air-water mixture, the remaining curve to be discussed is the one labeled a_1 and is, of course, from the new theory embodied in equation (32). The first figure shows that it is practically coincident with the ad hoc (M,s,2T) curve, a_2 , which, according to the results in Wallis (ref. 10) correlates the available experimental data about the minimum point. In figure 3 the a_1 curve subsequently deviates from the a_2 curve well past the minimum

point and intersects the a_3 curve at the pure gas side as both the a_1 and a_3 curves satisfy the gas boundary condition of isentropic propagation.

An insight into the mechanism explaining similar behavior for a_1 and a_2 at the minimum point and liquid boundary and different behavior at the gas boundary is obtained from figure 5, which plots the two-phase heat capacity ratio versus the void fraction. Bearing in mind that the minimum in the previous plots is located approximately at $\alpha = \frac{1}{2}$, this figure shows how the two-phase heat capacity ratio adjusts itself to an approximate value of unity in the minimum region from a void fraction of zero to about 0.95 before rising steeply to the pure gas value of $\gamma = 1.4$ at $\alpha = 1$. The approximate value of unity is needed for correspondence with isothermal sound propagation postulated in the (M,s,2T) model to fit the experimental points, and the 1.4 value is necessary to satisfy isentropic propagation in the pure gas phase.

One-Component Systems

With the new equation accomplishing the dual objective of correlating the minimum and boundary points for the air-water system, a comparative study was made for parahydrogen and nitrogen for which similar experimental data were unavailable. Both substances are in the cryogenic domain with nitrogen of primary interest because of its future role in the NTF program, and both are single-component two-phase systems. While steam and water also form a one-component system, this two-phase mixture will not be included in the comparative study. Instead, it is used to develop a thermodynamic criterion for determining if the (M,3s) theory can be correct

as implied by Semenov and Kosterin in reference 11 for steam and water.

Nitrogen

In the nitrogen study three plots similar to those shown for the air-water system were constructed for 80K, 100K, and 120K. These temperatures were arbitrarily selected to represent nitrogen's entire two-phase temperature range, $63.148 \text{ K} \leq T \leq 126.2 \text{ K}$. In addition, the (IHE) model was used to show a fourth velocity of sound designated as a_0 . Cryogenic tunnels such as NTF will normally have $\alpha \simeq 1$ and $x > 0.95$.

At the nitrogen temperature of 80K, which is furthest from the critical point, figures 6, 7, and 8 most closely resemble the three corresponding figures for the air-water system. The chief difference between one- and two-component systems as far as these figures are concerned is the γ_L value. For the air-water system it is close to unity while for nitrogen it is slightly greater than 2.1. This is shown in figures 5 and 8. The latter figure also shows the very rapid adjustment that the two-phase γ makes to values very close to unity for a large range of α (although not as large a range as that for the air-water system). Because of the rapid adjustment in γ , the minimum region of figure 6 shows a_1 and a_2 as being essentially one curve.

In figure 6 the (IHE) velocity of sound previously defined as a_0 is shown to be smaller than the minimum value of a_1 for a very large range of α before intersecting a_2 in the vicinity of $\alpha = 1$. This region is difficult to visualize because of the convergence of four

steeply rising curves; therefore, these curves are transformed by using the quality as the independent variable in figure 7. Here it is seen the a_0 curve intersects a_2 at an approximate quality of 0.3, and subsequently makes an apparently tangential contact with the a_1 curve at a quality of approximately 0.55. This tangential contact raises an interesting question about the meaning of points which appear to be simultaneously stable and metastable.

When the temperature of the nitrogen is changed to 100 K, the pattern associated with the previous three figures begins to shift a little although the basic features remain the same as seen in figures 9, 10, and 11. The a_1 and a_2 curves merge in a narrower minimum region of figure 9 with the minimum sound speed still being less than that predicted by the (M,3s) model. The narrowing of the merged region is accompanied by a more visible shift in the γ pattern as indicated by comparing figures 8 and 11. No longer is γ equal to one over a large fraction of the void fraction axis as in figure 8, even though it is still very close to one in its flat minimum region. Finally, the prior interaction and tangency characteristics of the equilibrium sound speed, a_0 , persist.

The variation in the triple pattern of plots becomes stronger when the temperature is shifted closer to the critical value for the final value of 120 K as seen in figures 12, 13, and 14. Now there is no region in figure 12 where the a_1 and a_2 curves merge. This strong change is accompanied by an equally strong shift in the γ pattern of figure 14 where no region exists for which γ can be approximated by unity. Therefore the (M,s,2T) model should not accurately predict the minimum region in this case because the necessary assumption of isothermal propagation is no longer valid.

Finally, the intersection and tangency characteristics in the a_0 curve persist, as is evident both in figures 12 and 13.

Parahydrogen

Parahydrogen has triple and critical temperatures of 13.803 K and 32.976 K (reference 13). From this range only the single temperature of 25 K was selected for the same kind of plots as before. This gives a reduced temperature of $\frac{T}{T_c} = 0.758$, which is very close to the reduced temperature of 0.792 for nitrogen at 100 K. From a principle of corresponding states view, it would be anticipated that figures 15, 16, and 17 for parahydrogen would be very similar to those for nitrogen as shown in figures 9, 10, and 11. This turns out to be only partially true. Figure 15 shows that while the a_1 and a_2 curves are very close together there is no region of overlap as is evident in the corresponding nitrogen figure 9. Subsequent comparison of figures 17 and 11 shows that γ for the parahydrogen has a narrower flat region about its minimum point which leads to a poorer approximation to the $\gamma = 1$ condition needed to merge the a_1 and a_2 curves in the vicinity of their minimum points.

Steam-Water

As a concluding part of this investigation, attention is now turned to the steam-water experiments of reference 11 which apparently support the triply isentropic model (M,3s) within the context of an uncertainty in sound speed measurement of $\pm 9\%$. The triple plots used in the comparative study of nitrogen and parahydrogen will be replaced by an analytical treatment involving the use of equations (9) and (10).

Since pressure and temperature equilibrium is assumed in the metastable models, the perturbation differentials dP and dT are the same for the liquid phase, the vapor phase, and the two-phase element. In the (M,3s) model $ds = ds_L = ds_G = 0$. Applying these assumptions to equation (9) and (10) gives the perturbation pressure-temperature ratio dP/dT as

$$\frac{dP}{dT} = \frac{C_{P,L}}{T} \left(\frac{\partial T}{\partial v} \right)_{P,L} \quad (36)$$

and

$$\frac{dP}{dT} = \frac{C_{P,G}}{T} \left(\frac{\partial T}{\partial v} \right)_{P,G} \quad (37)$$

Equating the two expressions for dP/dT gives

$$C_{P,L} \left(\frac{\partial T}{\partial v} \right)_{P,L} = C_{P,G} \left(\frac{\partial T}{\partial v} \right)_{P,G} \quad (38)$$

which will be used in a nondimensional ratio form, r , by defining

$$r = \frac{C_{P,L}}{C_{P,G}} \left(\frac{\partial T}{\partial v} \right)_{P,L} \left(\frac{\partial v}{\partial T} \right)_{P,G} \quad (39)$$

where, of course,

$$r = 1 \quad (40)$$

This result is important in that the postulates of the (M,3s) model predict a property law which can be checked by using suitable tables of thermodynamic properties. For the steam-water system it was checked by using the properties found in table 1 of reference 11, and by transforming r to accommodate them. This is accomplished by rearranging the thermodynamic single-phase equation for the difference in specific heat capacities to

$$\left(\frac{\partial v}{\partial T} \right)_P = \sqrt{\frac{C_P - C_v}{T} \left\{ -\frac{1}{v} \left(\frac{\partial v}{\partial P} \right)_T \right\}_v} \quad (41)$$

Applying this successively to the liquid phase and to the gas phase and then substituting both into equation (39) gives

$$r = \frac{C_{P,L}}{C_{P,G}} \sqrt{\frac{(C_P - C_V)_G}{(C_P - C_V)_L} \frac{\left\{ -\frac{1}{v} \left(\frac{\partial v}{\partial P} \right)_T \right\}_G v_G}{\left\{ -\frac{1}{v} \left(\frac{\partial v}{\partial P} \right)_T \right\}_L v_L}} \quad (42)$$

Introduction of the tabulated data from reference 11 gives the following results for steam-water at four saturation temperatures:

T(K)	r
452.2	746
470.5	461
484.5	318
522.3	112

Since r fails to satisfy equation (40) the conclusion, based on the equations developed in this paper, is that the (M,3s) theory is invalid and that the +9% uncertainty in the steam-water sound speed measurements of reference 11 is sufficient to conceal this.

In the case of the air-water system it is known that the (M,3s) model does not fit the experimental data. From the above analysis it would be expected that $r \neq 1$ and indeed the computation gives $r = 84300$.

For parahydrogen experimental data is lacking for the required sound speed curve. Falling back on the r computation gives $r = 39.3$ which invalidates the (M,3s) model in the context of the theory of this paper.

A similar conclusion is drawn for nitrogen where, again, experimental data for the sound speed curve are lacking; for, at the three temperatures 80K, 100K, and 120K, the respective values of r were calculated as 580, 64.4, and 7.80.

SUMMARY OF RESULTS

A new method of calculating speed of sound for two-phase flow has been presented. The new equation assumes no phase change during the propagation of an acoustic disturbance and assumes that only the total entropy of the mixture remains constant during the process. It is shown that the new equation predicts single-phase values for the speed of sound in the limit of all gas or all liquid and agrees with available two-phase, air-water sound speed data. Other expressions used in the two-phase flow literature for calculating two-phase, metastable sound speed are reviewed and discussed. Comparisons are made between the new expression and several of the previous expressions -- most notably a triply isentropic equation as used, among others, by Karplus and by Wallis. Appropriate differences are pointed out and a thermodynamic criterion is derived which must be satisfied in order for the triply isentropic expression to be thermodynamically consistent. This criterion is not satisfied for the cases examined, which included two-phase nitrogen, air-water, two-phase parahydrogen, and steam-water. Consequently, the new equation derived is found to be superior to the other equations reviewed.

The importance of this work to cryogenic wind tunnels is that it properly defines the two-phase speed of sound to use as the mixture approaches the limit of all gas. In particular, the correct speed of sound approaches the single-phase gas velocity of sound and not a value substantially less as predicted by an isothermal formulation. In other words, in regions of small amounts of liquid mixed with gas (vapor mass fraction greater than 0.98), the speed of sound will be very close to that value expected for single-phase flow.

REFERENCES

1. Kilgore, Robert A.: The Cryogenic Wind Tunnel for High Reynolds Number Testing. Ph.D. Thesis, University of Southampton, 1974.
2. Polhamus, Edward C.; Kilgore, Robert A.; Adcock, Jerry B.; and Ray, Edward J.: The Langley Cryogenic High Reynolds Number Wind-Tunnel Program. *Astronautics and Aeronautics*, October, 1974, pp. 30-40.
3. McKinney, Linwood W.; and Howell, Robert R.: The Characteristics of the Planned National Transonic Facility. Presented at the AIAA Ninth Aerodynamic Testing Conference, Arlington, Texas, June 7-9, 1976.
4. Adcock, Jerry B.: Real-Gas Effects Associated with One-Dimensional Transonic Flow of Cryogenic Nitrogen. NASA TN D-8274, 1976.
5. Hall, Robert M.: Onset of Condensation Effects with a NACA 0012-64 Airfoil Tested in the Langley 0.3-meter Cryogenic Tunnel. NASA TM 78666, 1978.
6. Jacobsen, R. T.: The Thermodynamic Properties of Nitrogen from 65 to 2000 K with Pressures to 10,000 Atm. Ph.D. Thesis, Washington State Univ., 1972.
7. Karplus, H. B.: The Velocity of Sound in a Liquid Containing Gas Bubbles. Rep. C00-248, Armour Res. Found., June 1958.
8. Wood, A. B.: A Textbook of Sound. McGraw-Hill Book Co., 1955, p. 361.
9. Dvornichenko, V. V.: Influence of Fluid Compressibility on the Sonic Velocity in a Steam-Liquid Mixture in the Two-Phase Region. *Teploenergetika*, 1969, 16(4), pp. 68-71.

10. Wallis, G. B.: One-Dimensional Two-Phase Flow. McGraw-Hill Book Co., 1969.
11. Semenov, N. I.; and Kosterin, S. I.: Results of Studying the Speed of Sound in Moving Gas-Liquid Systems. Teploenergetika, 1964, 11, (6) pp. 46-51.
12. Epstein, P. S.; and Carhart, R. R.: The Absorption of Sound in Suspensions and Emulsions. I. Water Fog in Air. Journ. of the Acoust. Soc. Amer., 1953, 25, (3) pp 553-565.
13. Weber, L. A.: Thermodynamic and Related Properties of Parahydrogen From the Triple Point to 300 K at Pressures to 1000 Bar. NASA SP-3088 and NBSIR 74-374, 1975.

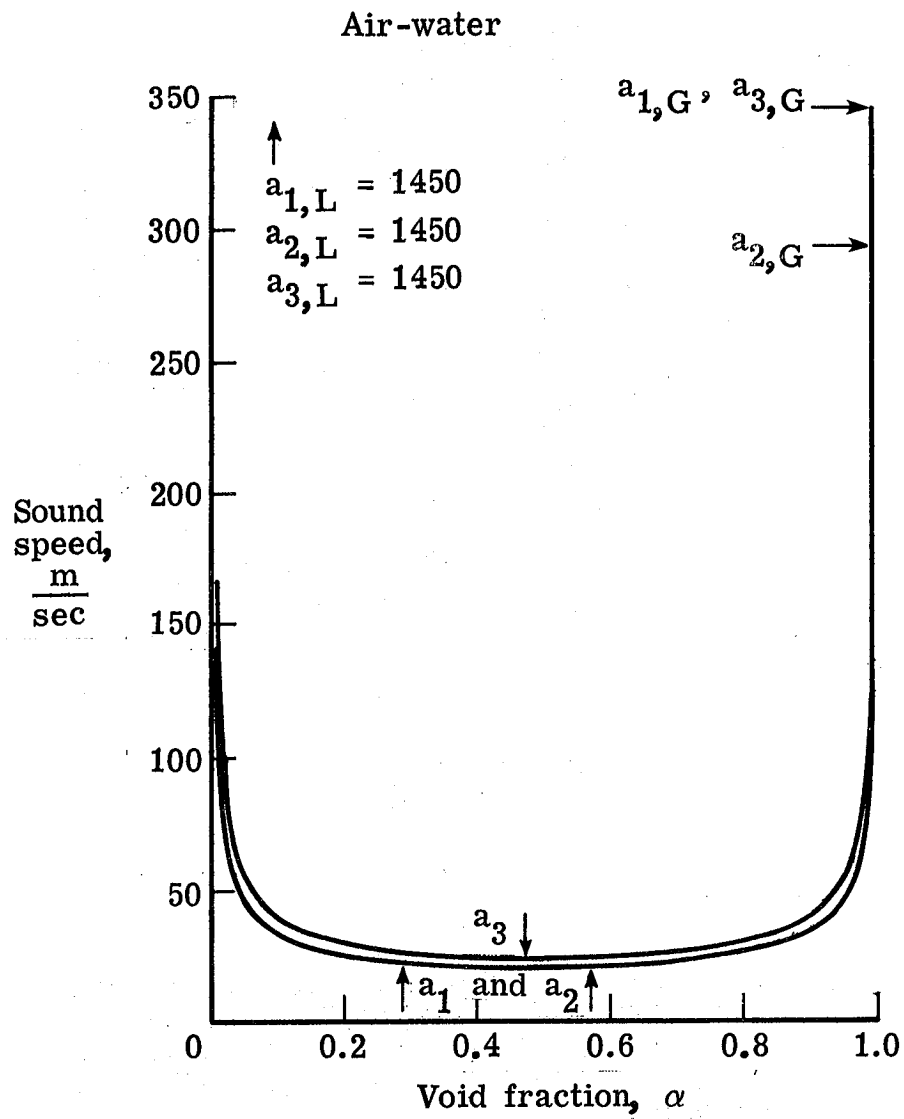


Figure 1.- Different sound speeds for an air-water system at 290 K as a function of void fraction.

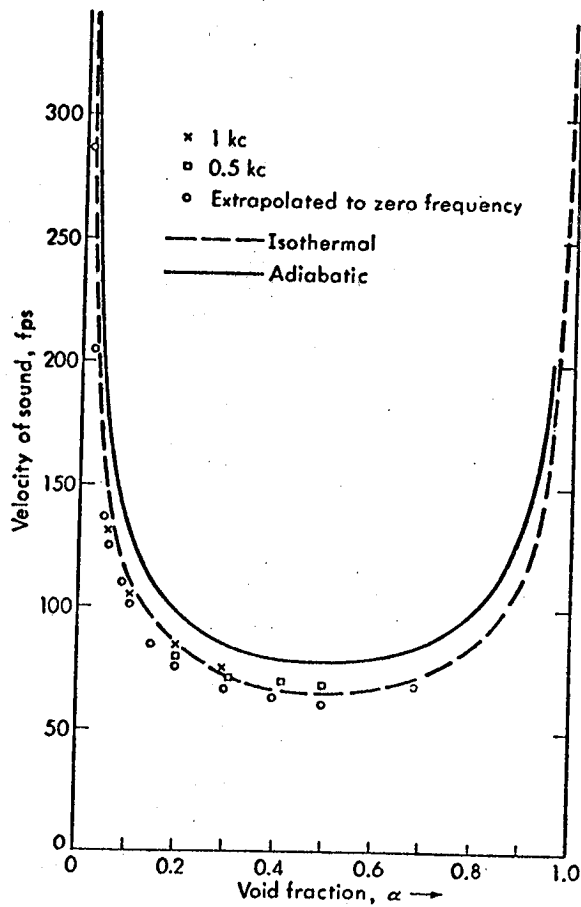


Figure 2.- Experimental and theoretical sound speeds for a mixture of air and water at atmospheric conditions. The isothermal line corresponds to a_2 and the adiabatic line corresponds to a_3 . This figure is from One-Dimensional Two-Phase Flow by Wallis. Copyright (c) 1969 by McGraw-Hill, Incorporated. Used with permission of McGraw-Hill Book Company.

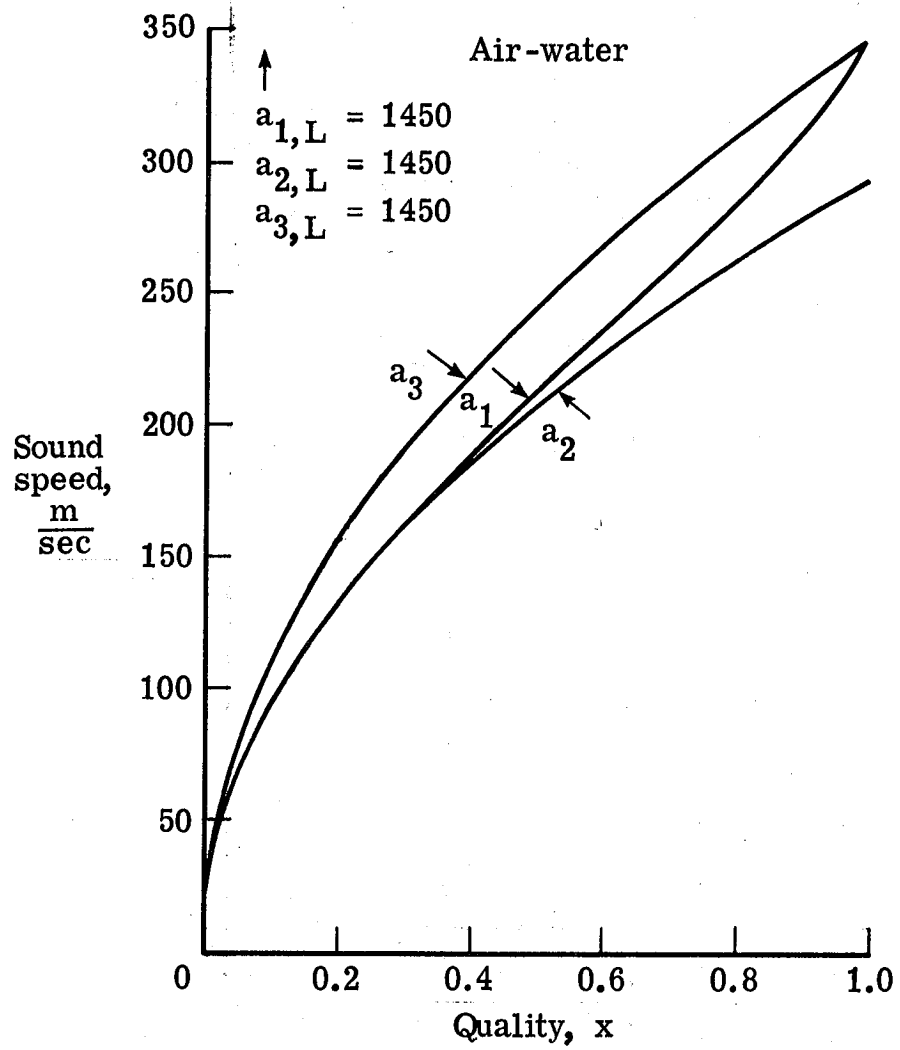
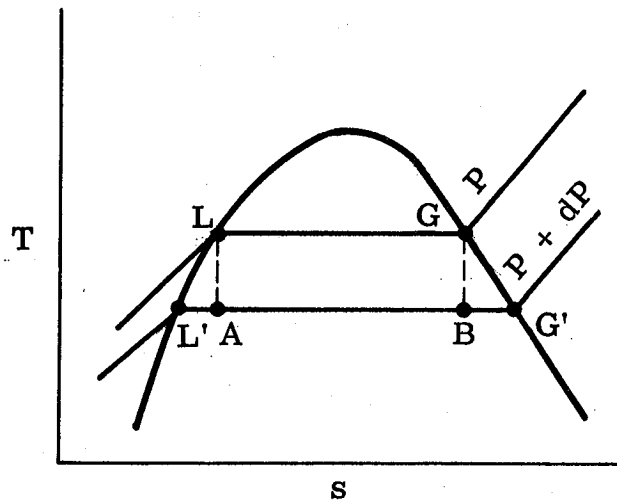
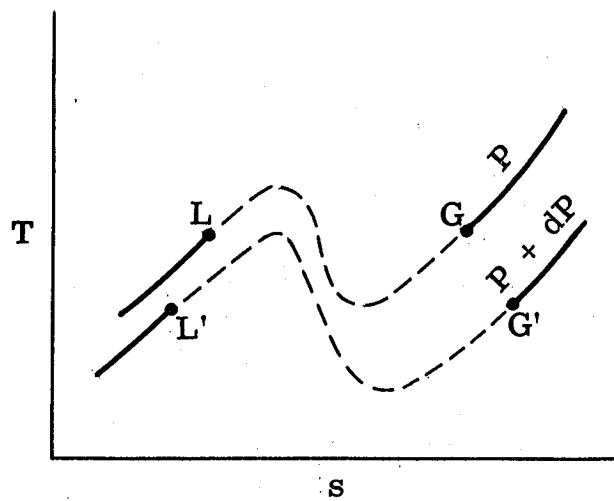


Figure 3.- Different sound speeds for an air-water system at 290 K as a function of quality.



(a) Equilibrium description.



(b) Metastable description.

Figure 4.- Description of metastability on thermodynamic properties.

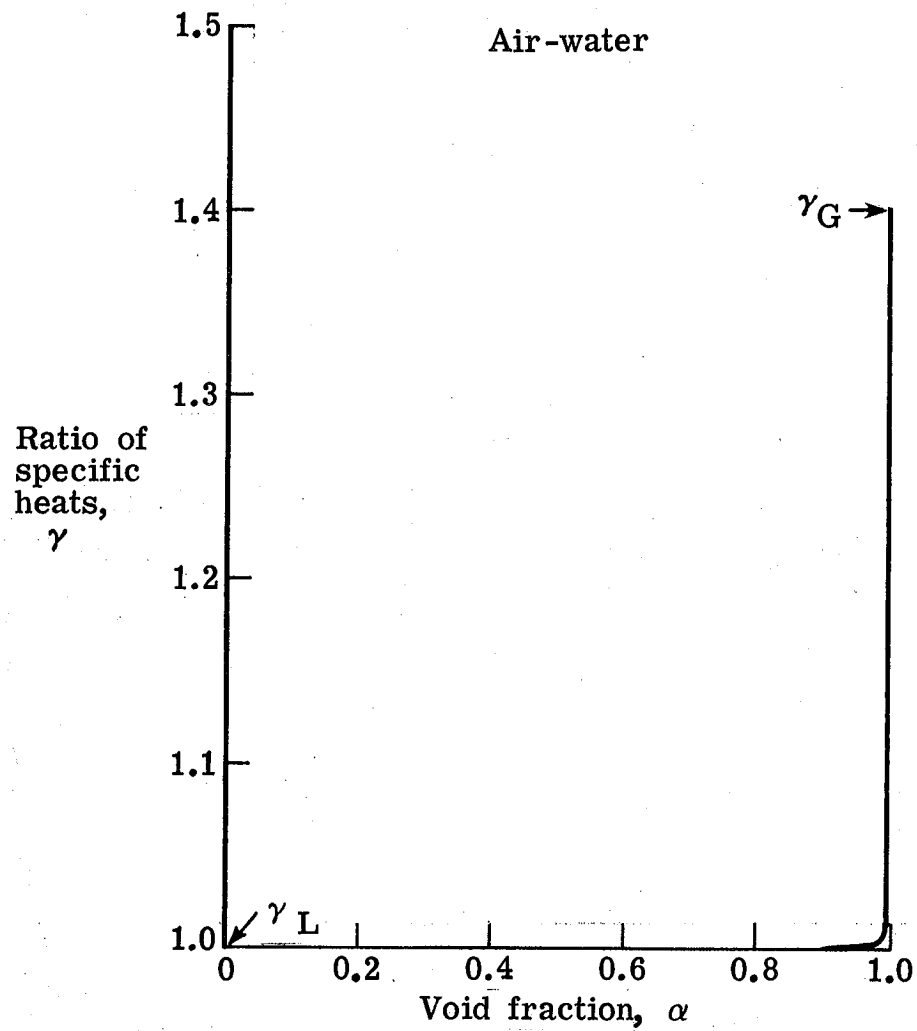


Figure 5.- Ratio of specific heats for an air-water system at 290 K.

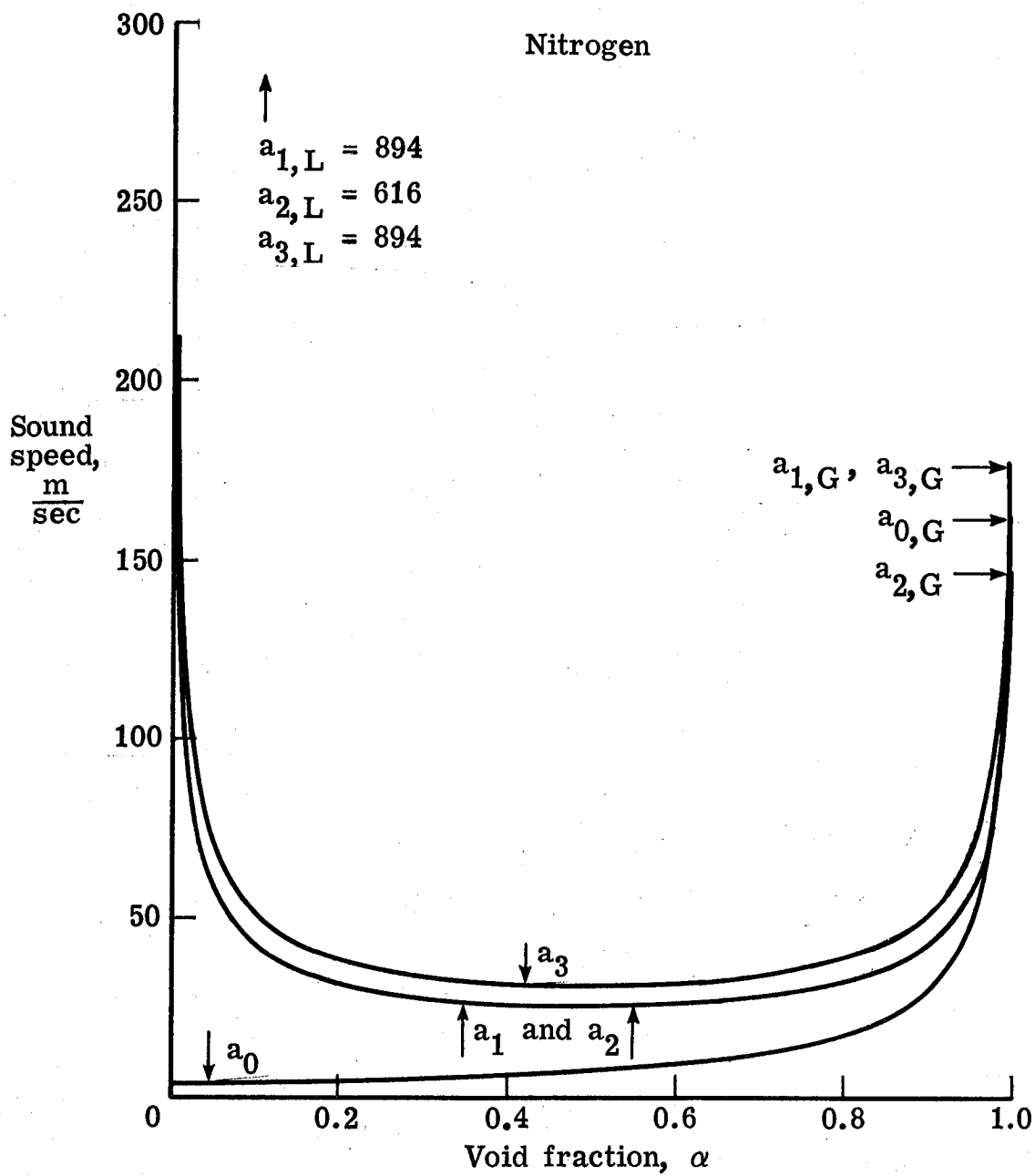


Figure 6.- Different sound speeds for two-phase nitrogen at 80 K as a function of void fraction.

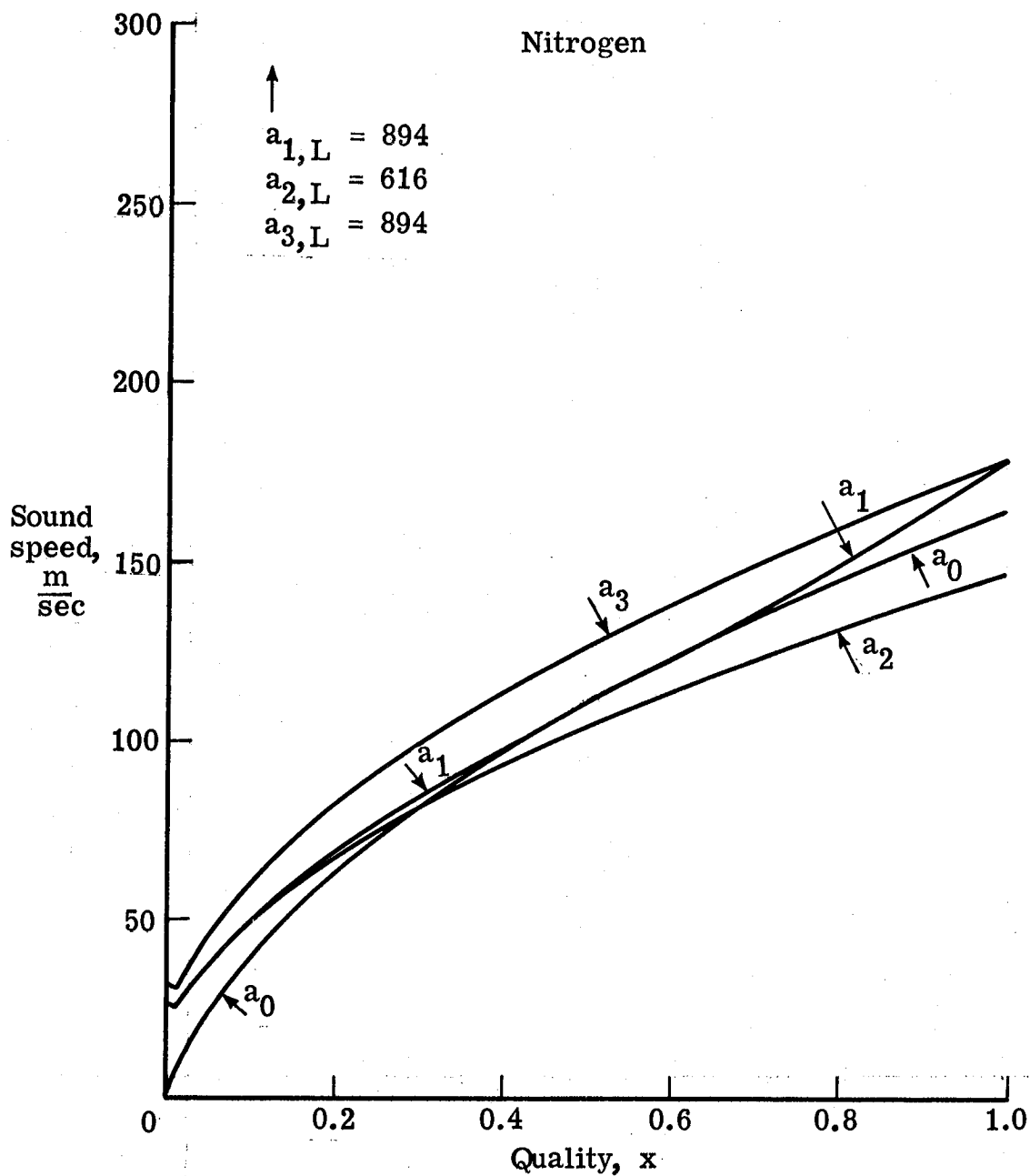


Figure 7.- Different sound speeds for two-phase nitrogen at 80 K as a function of quality.

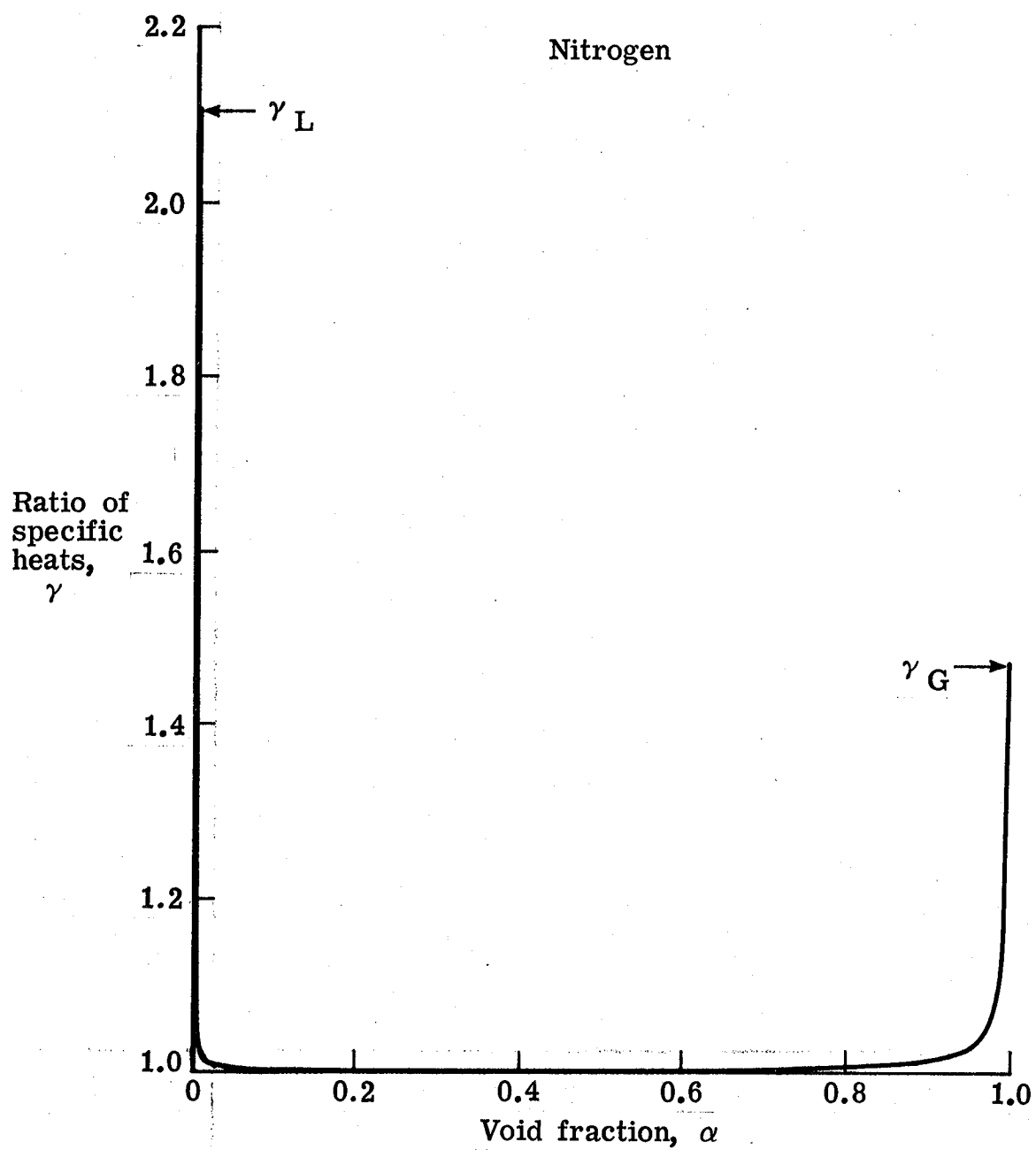


Figure 8.- Ratio of specific heats for two-phase nitrogen at $T = 80$ K.

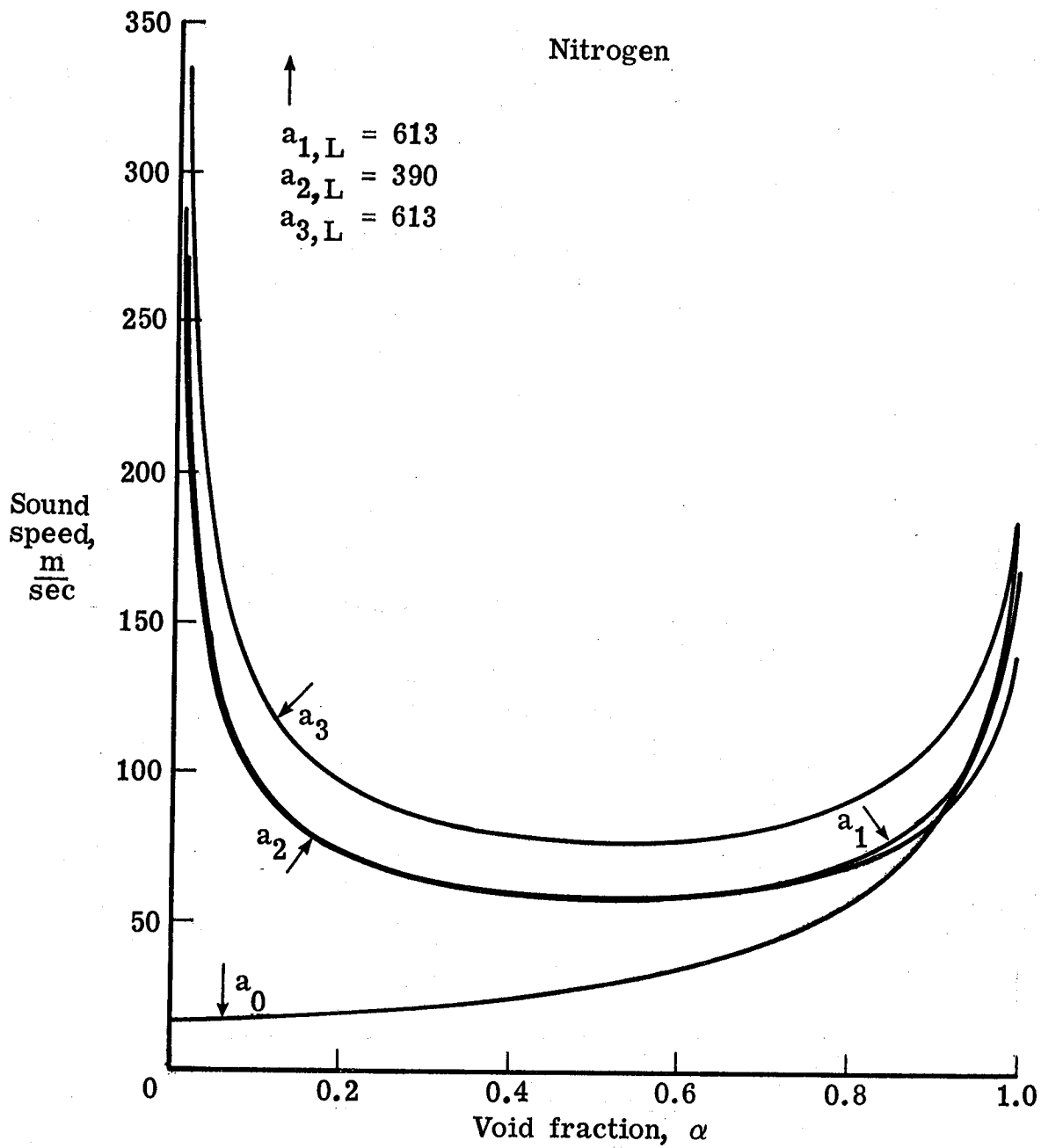


Figure 9.- Different sound speeds for two-phase nitrogen at $T = 100$ K as a function of void fraction.

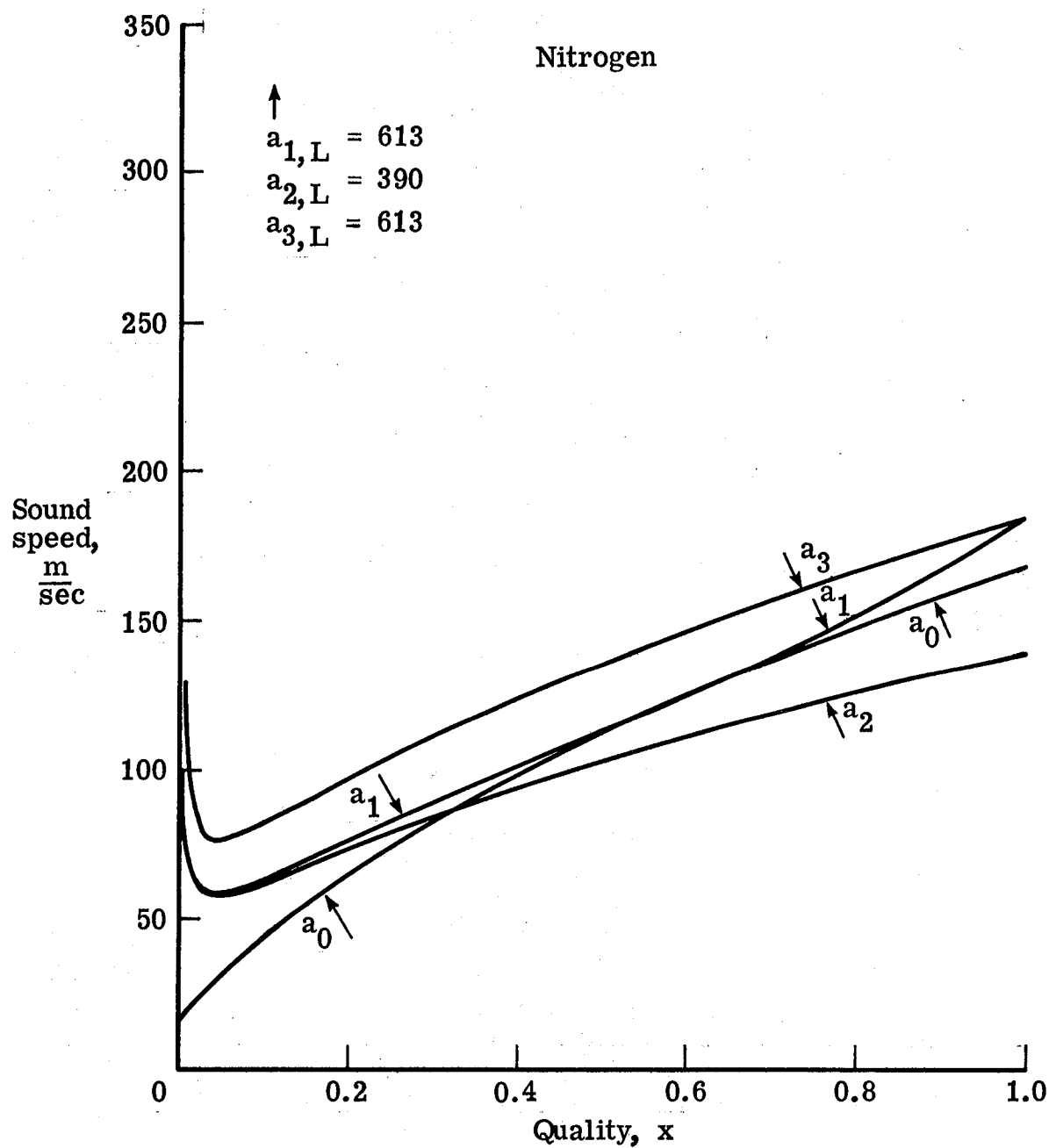


Figure 10.- Different sound speeds for two-phase nitrogen at 100 K as a function of quality.

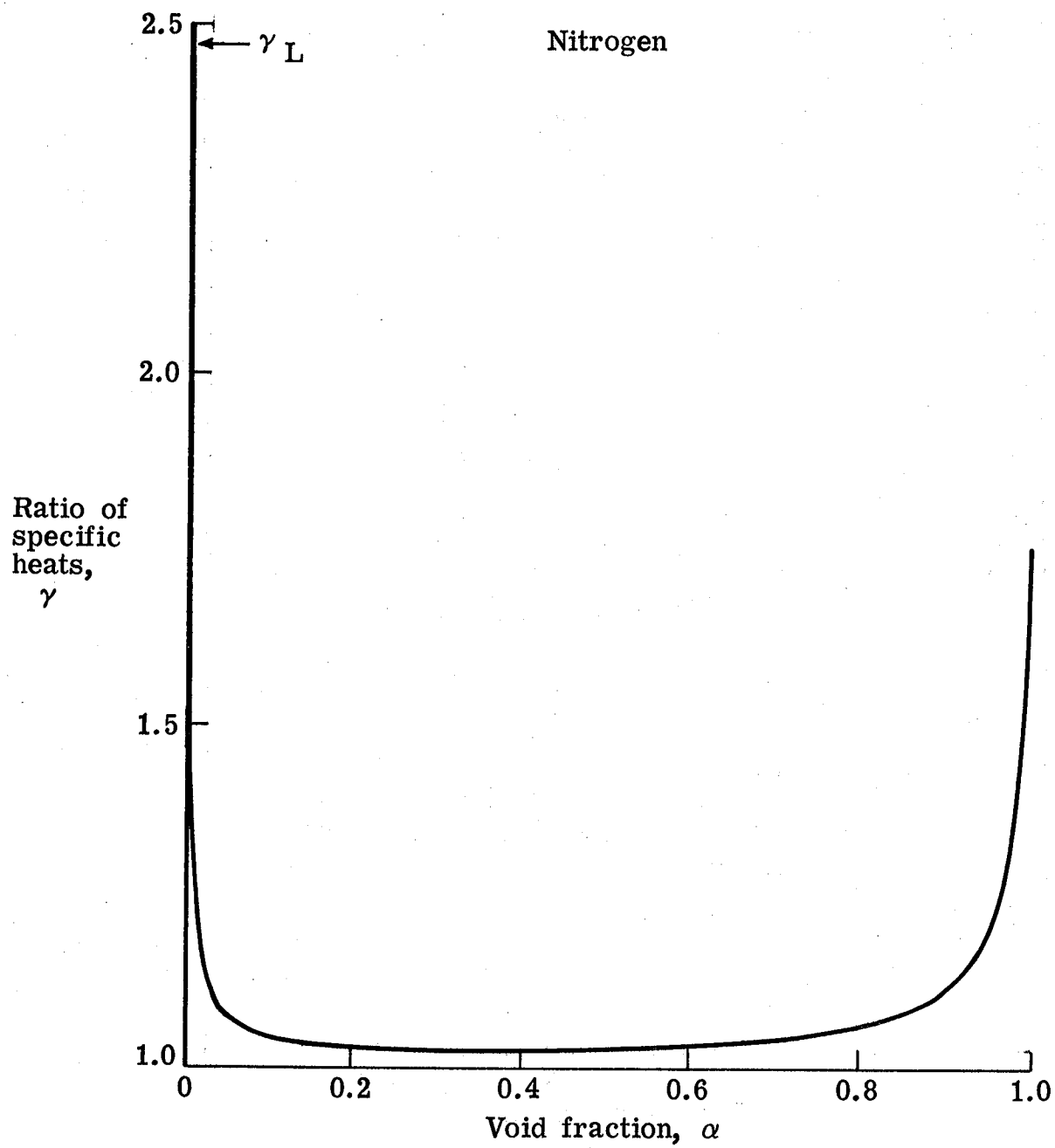


Figure 11.- Ratio of specific heats for two-phase nitrogen at $T = 100$ K.

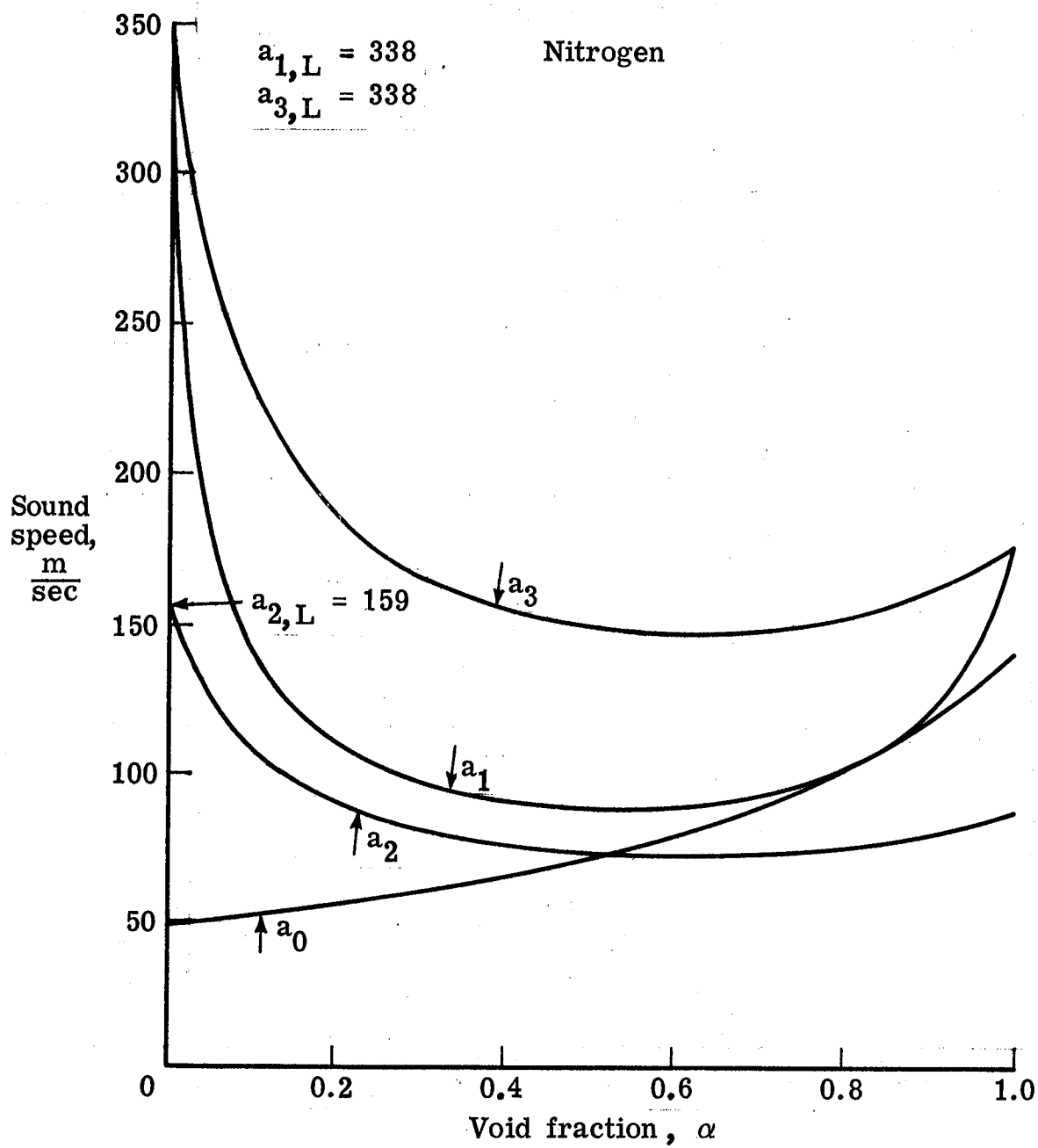


Figure 12.- Different sound speeds for two-phase nitrogen at $T = 120$ K as a function of void fraction.

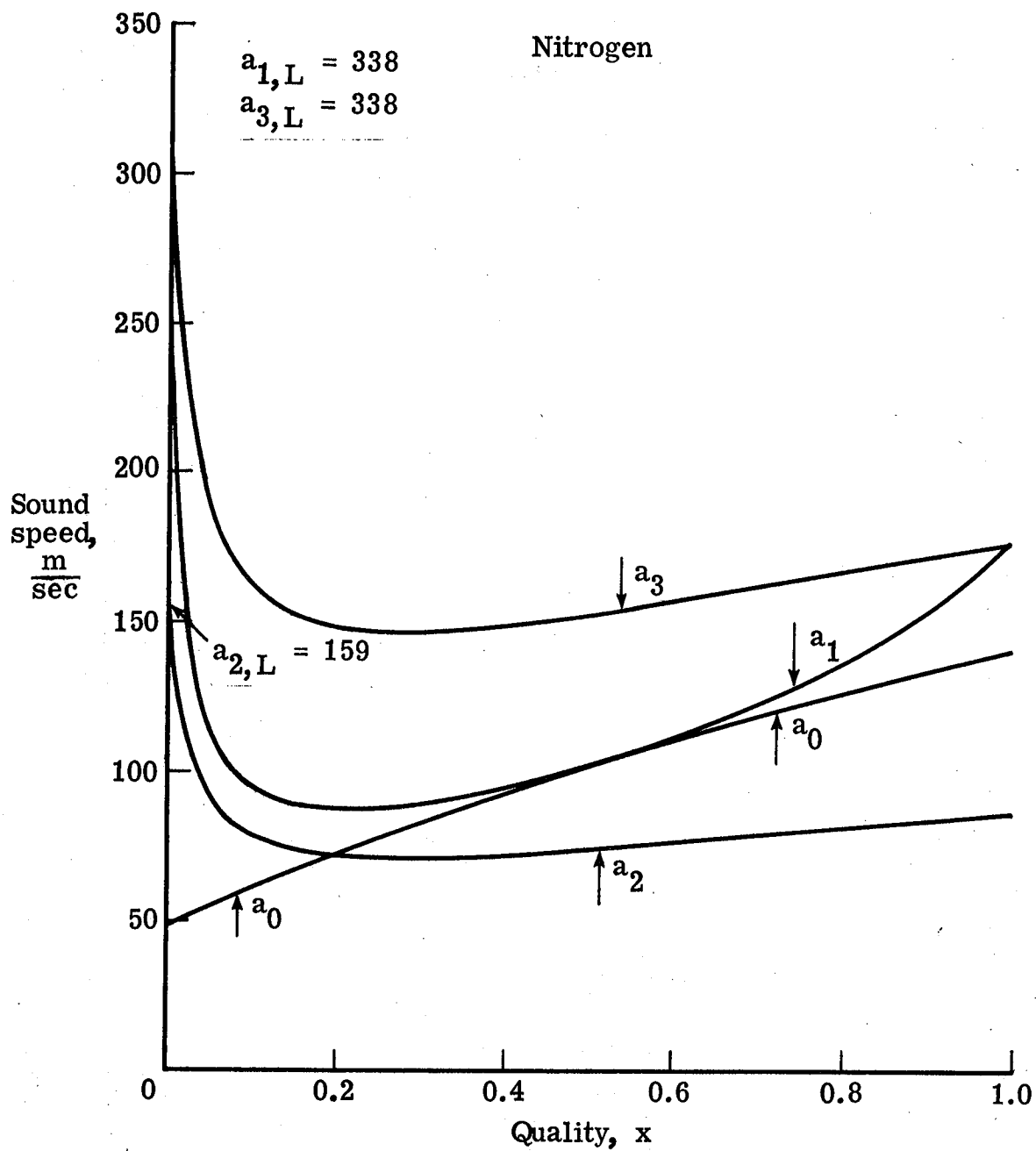


Figure 13.- Different sound speeds for two-phase nitrogen at 120 K as a function of quality.

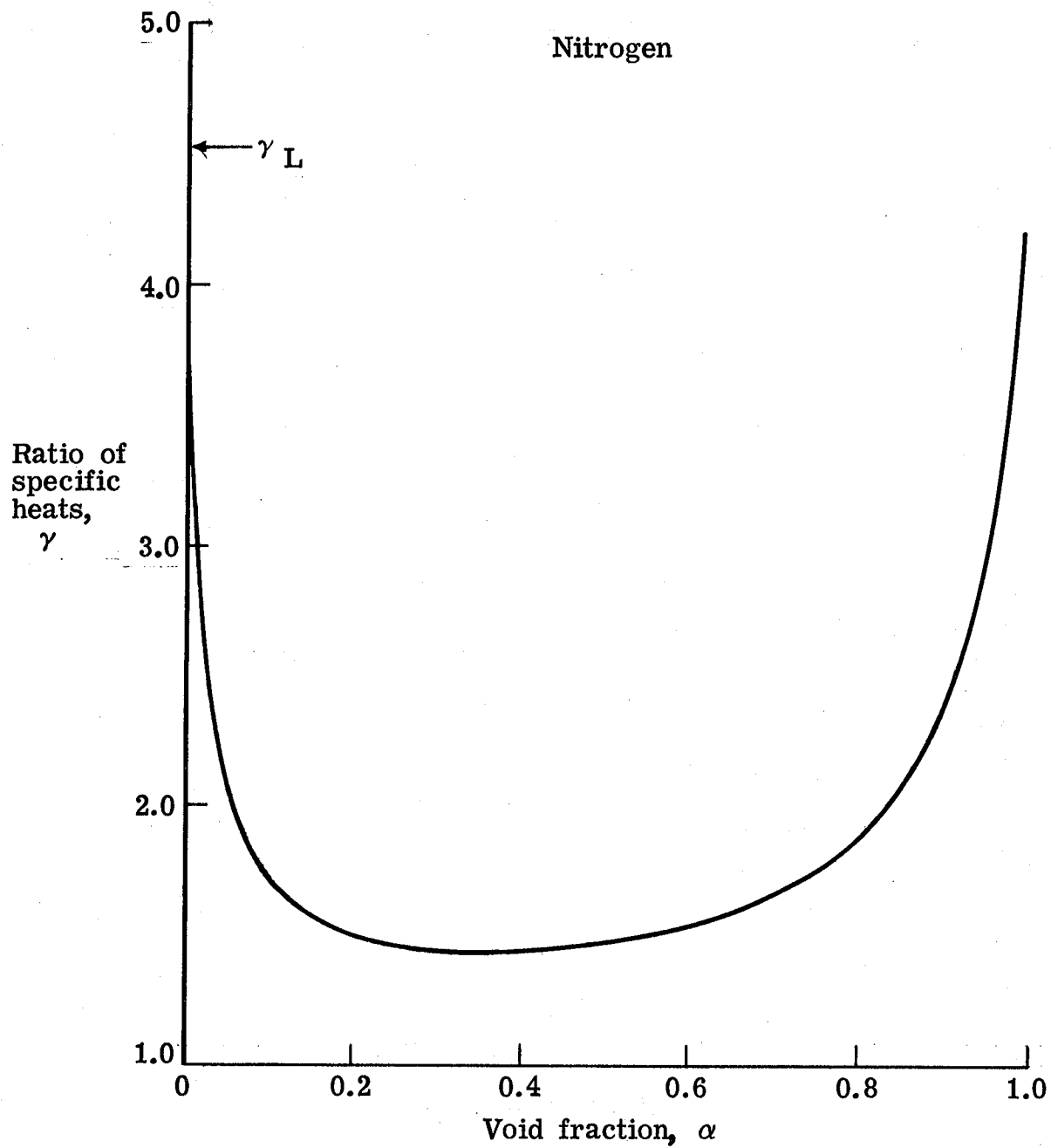


Figure 14.- Ratio of specific heats for two-phase nitrogen at $T = 120$ K.

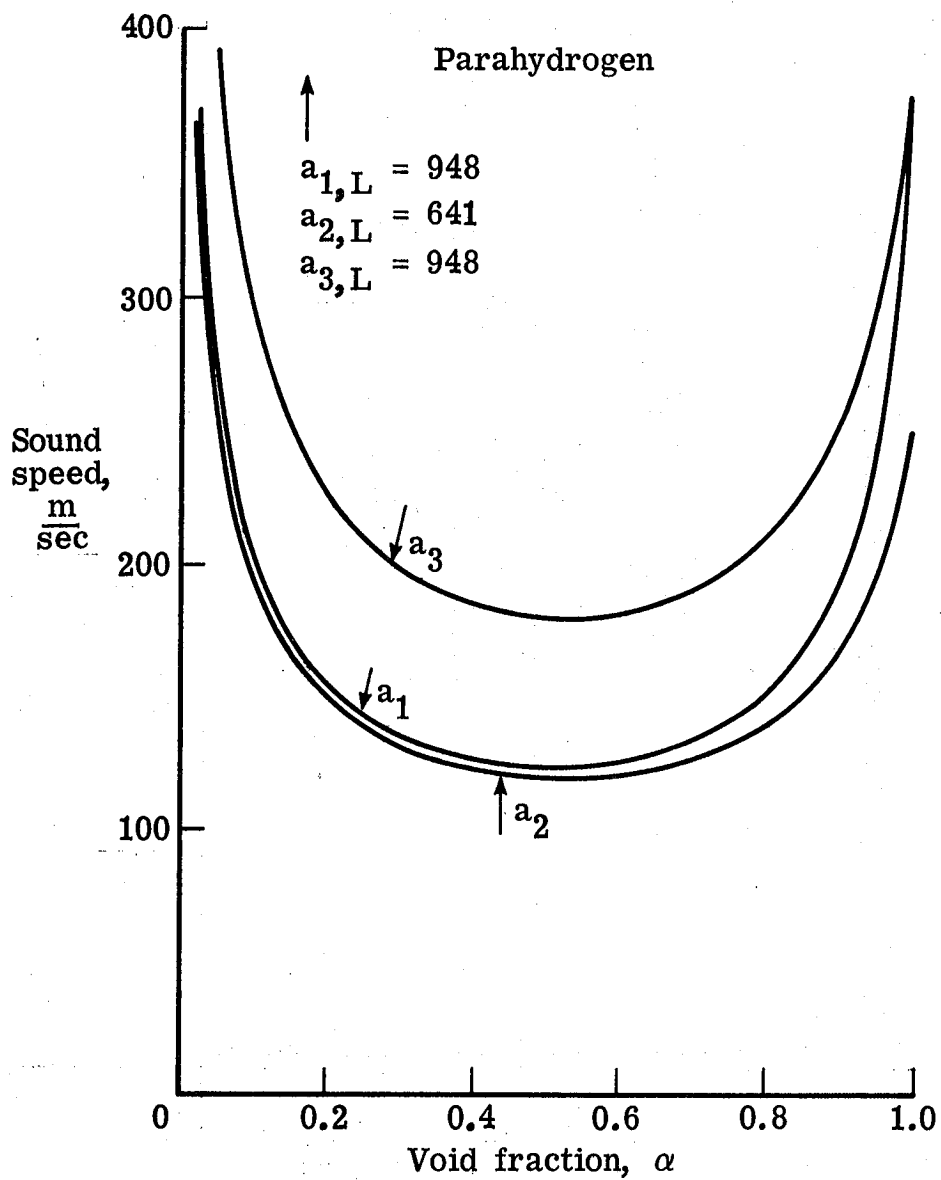


Figure 15.- Different sound speeds for two-phase parahydrogen at $T = 25$ K as a function of void fraction.

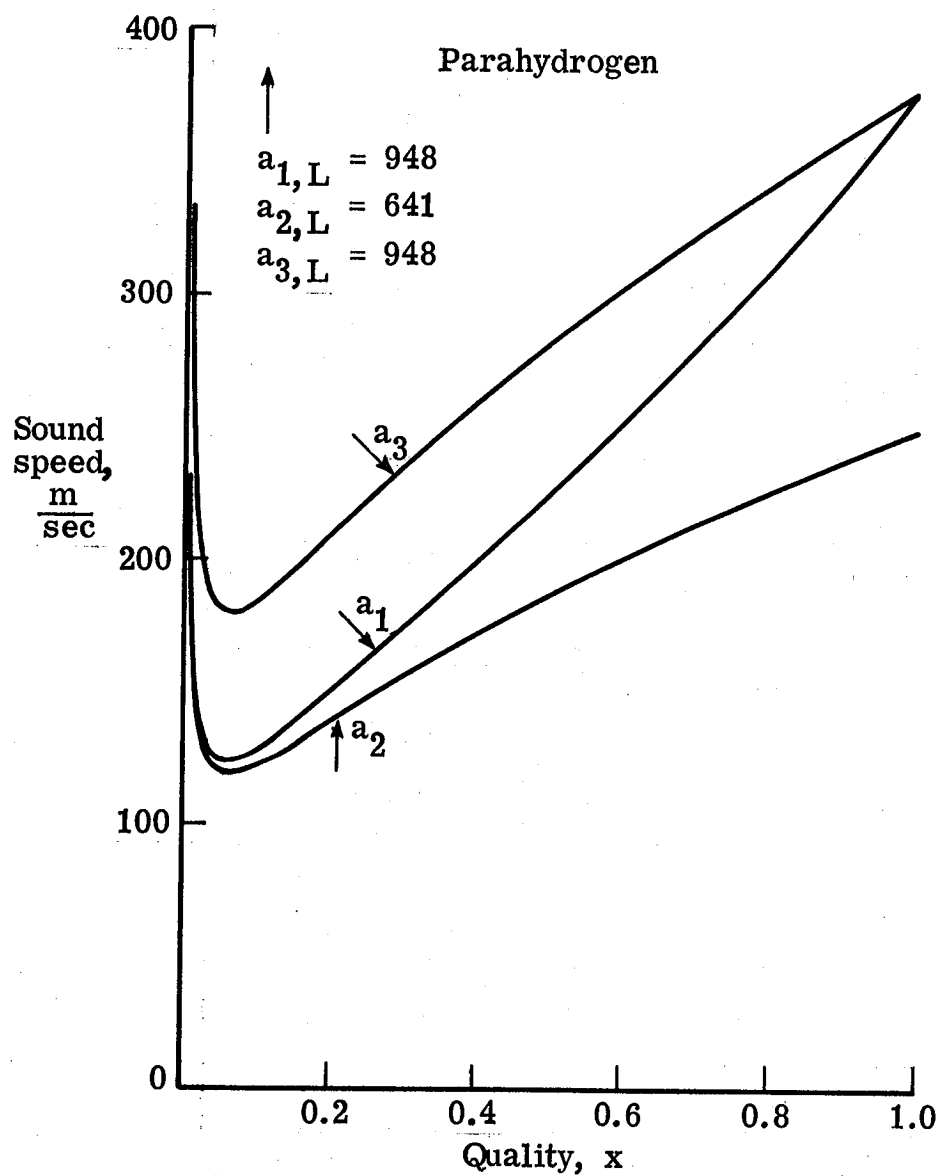


Figure 16.- Different sound speeds for two-phase parahydrogen at $T = 25$ K as a function of quality.

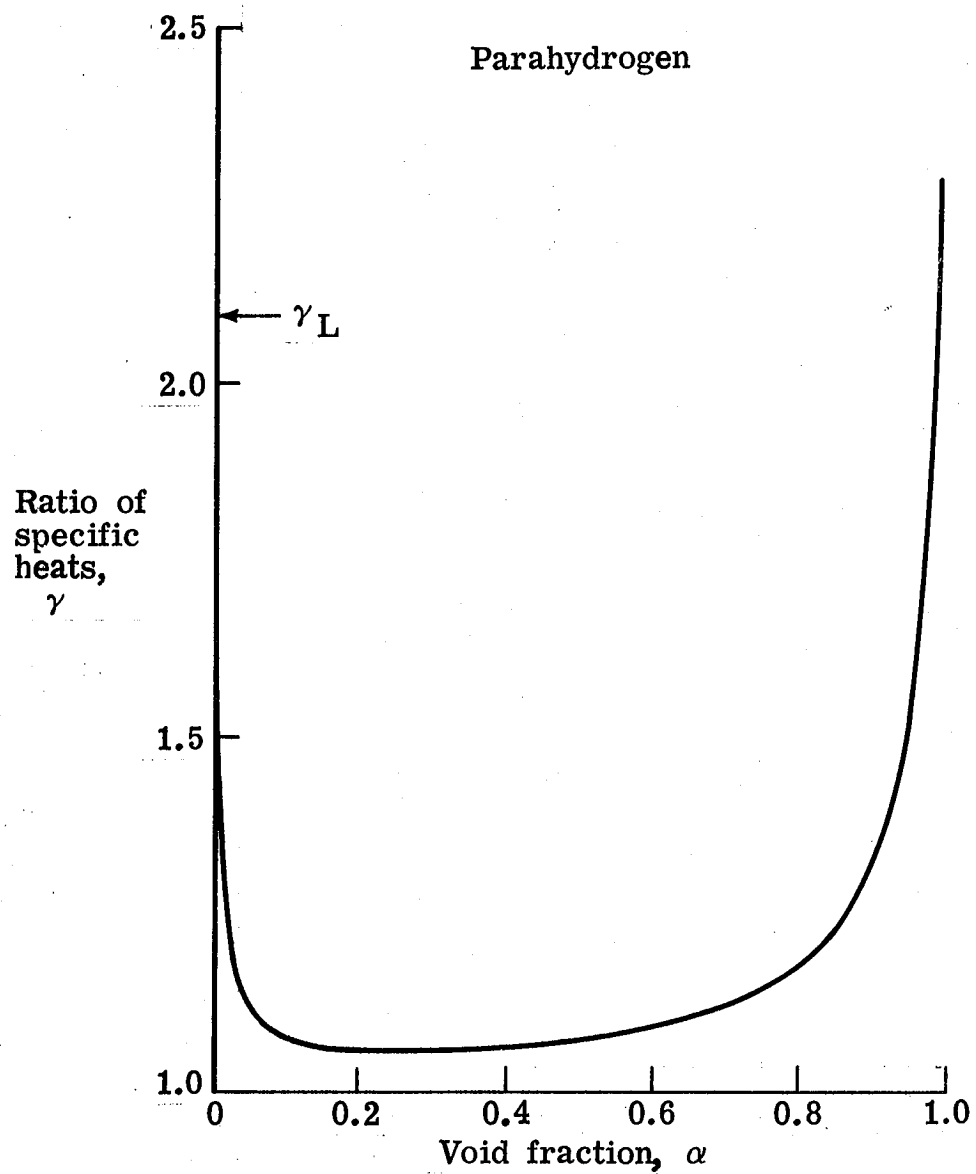


Figure 17.- Ratio of specific heats for two-phase parahydrogen at $T = 25$ K.

1. Report No. TM 78810		2. Government Accession No.		3. Recipient's Catalog No.	
4. Title and Subtitle METASTABLE SOUND SPEED IN GAS-LIQUID MIXTURES				5. Report Date March 1979	
				6. Performing Organization Code 505-06-43-08	
7. Author(s) Joseph W. Bursik* and Robert M. Hall				8. Performing Organization Report No.	
9. Performing Organization Name and Address NASA Langley Research Center Hampton, Virginia 23665				10. Work Unit No.	
				11. Contract or Grant No.	
12. Sponsoring Agency Name and Address National Aeronautics and Space Administration Washington, DC 20546				13. Type of Report and Period Covered Technical Memorandum	
				14. Sponsoring Agency Code	
15. Supplementary Notes *Associate Professor of the Mechanical Engineering, Aeronautical Engineering and Mechanics, Rensselaer Polytechnic Institute, Troy, New York					
16. Abstract A new method of calculating speed of sound for two-phase flow is presented. The new equation assumes no phase change during the propagation of an acoustic disturbance and assumes that only the total entropy of the mixture remains constant during the process. The new equation predicts single-phase values for the speed of sound in the limit of all gas or all liquid and agrees with available two-phase, air-water sound speed data. Other expressions used in the two-phase flow literature for calculating two-phase, metastable sound speed are reviewed and discussed. Comparisons are made between the new expression and several of the previous expressions -- most notably a triply isentropic equation as used, among others, by Karplus and by Wallis. Appropriate differences are pointed out and a thermodynamic criterion is derived which must be satisfied in order for the triply isentropic expression to be thermodynamically consistent. This criterion is not satisfied for the cases examined, which included two-phase nitrogen, air-water, two-phase parahydrogen, and steam-water. Consequently, the new equation derived is found to be superior to the other equations reviewed.					
17. Key Words (Suggested by Author(s)) Speed of sound Two-phase flow Cryogenic wind tunnels Nitrogen			18. Distribution Statement Unclassified - Unlimited Star Category - 34		
19. Security Classif. (of this report) Unclassified	20. Security Classif. (of this page) Unclassified	21. No. of Pages 52	22. Price* \$5.25		

